PNAS
www.pnas.org

Supplementary Information for

Regulation of spatio-temporal limits of developmental gene expression via enhancer grammar

Samuel H. Keller[a,1], Siddhartha G. Jena[b,1], Yuji Yamazaki[c], Bomyi Lim[a]*

[a]Department of Chemical and Biomolecular Engineering, University of Pennsylvania, Philadelphia, PA 19104

[b]Department of Molecular Biology, Princeton University, Princeton, NJ 08544

[c]Yutaka Seino Distinguished Center for Diabetes Research, Kansai Electric Power Medical Research Institute, Kobe Japan

[1]S.H.K. and S.G.J. contributed equally to this work

*To whom correspondence may be addressed:

bomyilim@seas.upenn.edu

This PDF file includes:

Figures S1 to S3
Table S1
Legends for Movies S1 to S4

Other supplementary materials for this manuscript include the following:

Movies S1 to S4

www.pnas.org/cgi/doi/10.1073/pnas.1917040117

Figure S1

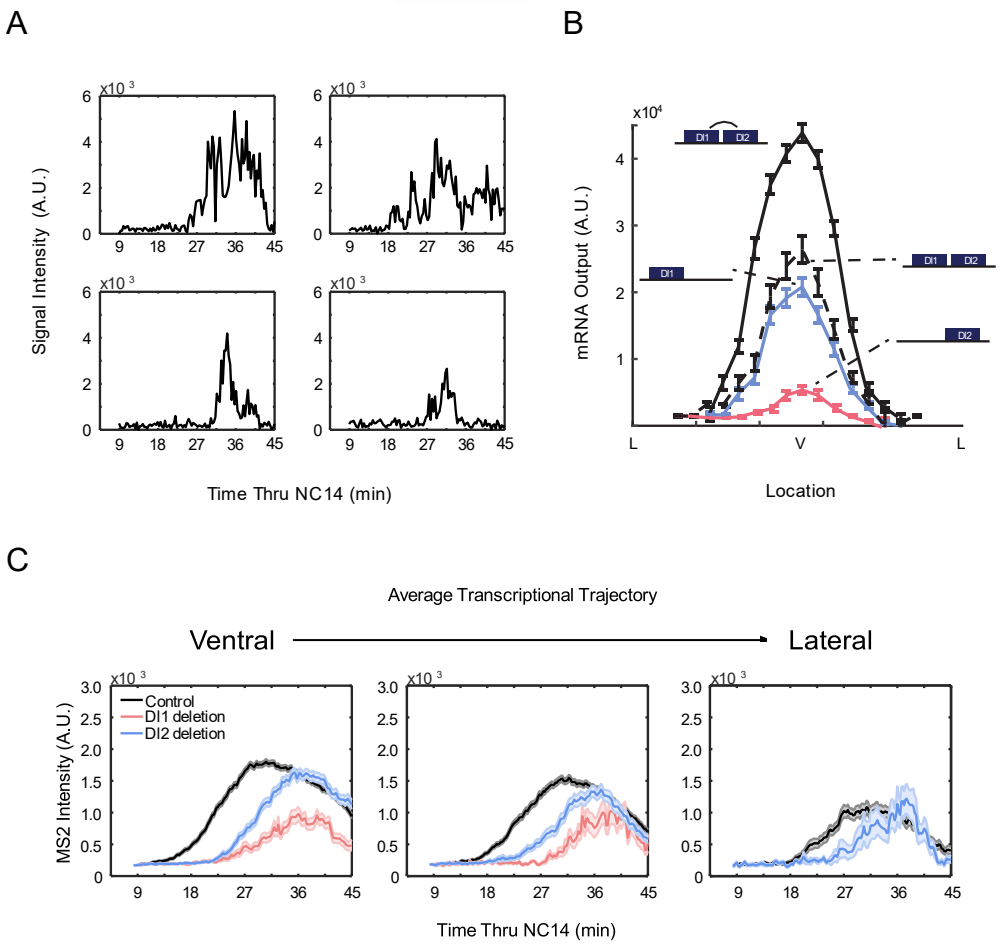

(A) MS2 trajectories of four randomly picked nuclei of a *t48-Dl1deletion>MS2-yellow* embryo.
(B) Measurement of the total *t48>MS2-yellow* mRNA production at different points along the DV axis, with the TF binding site modifications shown. Deletion of Dl1 site (red) or Dl2 site (blue) results in weaker expression of *MS2-yellow* than the expression driven by the wild type *t48* enhancer (black). Synergy between TF binding sites is revealed since the sum of transcriptional activity from single binding site alone (dashed black) is lower than the wild type.
(C) Average trajectory of *t48-WT>MS2-yellow* (black), *t48-Dl1deletion>MS2-yellow* (red), and *t48-Dl2deletion>MS2-yellow* (blue) over NC14 of ventrally located nuclei (left), off-ventral nuclei (center), and lateral nuclei (right).

Figure S2

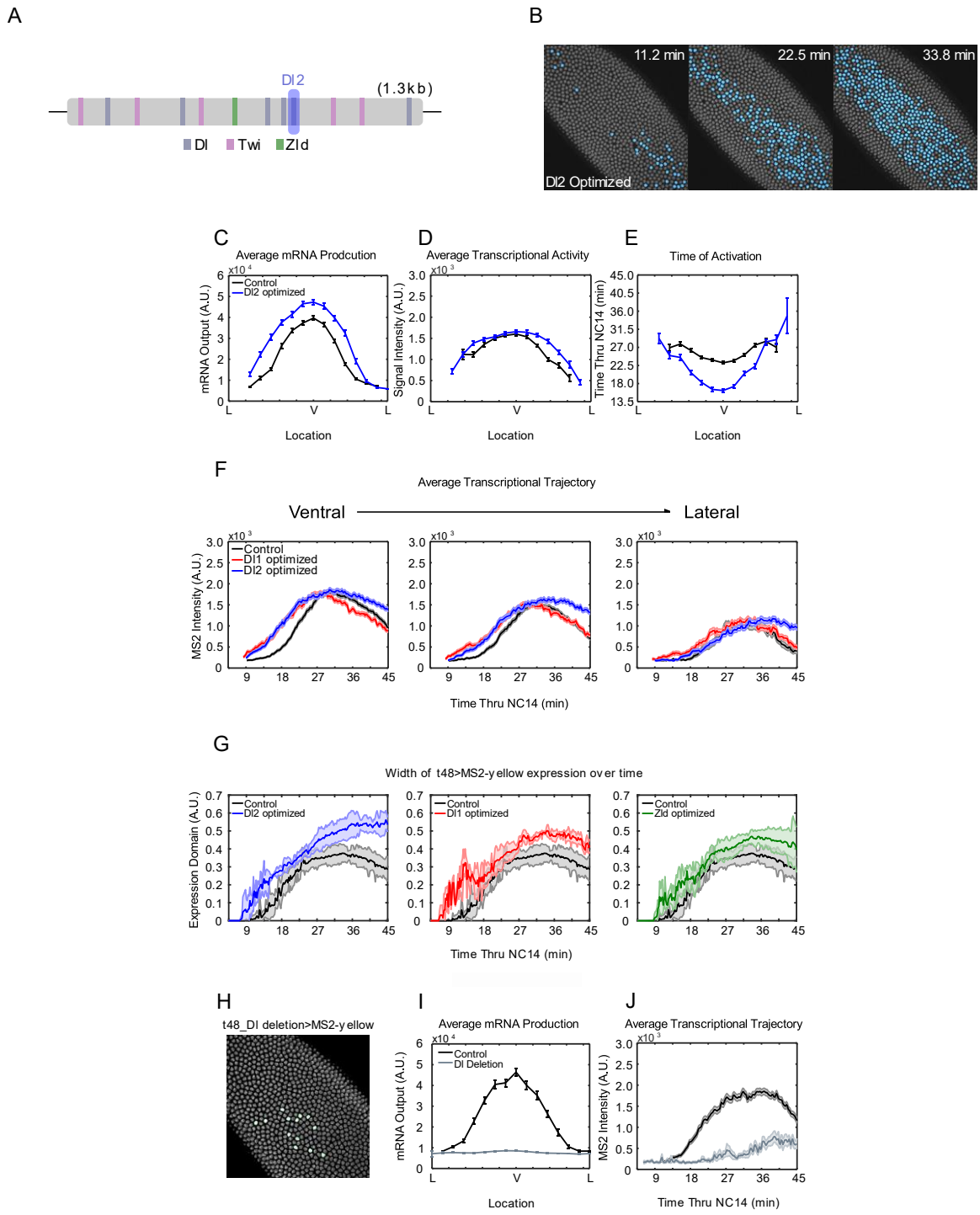

(A) Schematic of *t48* enhancer showing the location of Dl, Twi, and Zld binding sites. The Dl2 site is shown in blue.

(B) Snapshots of *t48-optimizedDl2>MS2-yellow* embryo at different time points in NC14. Actively transcribing nuclei in a given frame are false-colored.

(C-E) (C) Average total mRNA production, (D) average transcriptional intensity, and (E) average timing of transcriptional initiation of nuclei along the *t48* expression domain for *t48-WT>MS2-yellow* (black), *t48-optimizedDl2>MS2-yellow* (blue). Only active nuclei were analyzed for (D), (E), and (F). 1840 nuclei were examined from three biological replicate embryos of *t48-optimizedDl2>MS2-yellow* embryos.
(F) Average trajectory of *t48-WT>MS2-yellow* (black), *t48-optimizedDl1>MS2-yellow* (red), and *t48-optimizedDl2>MS2-yellow* (blue) over NC14 of ventrally located nuclei (left), off-ventral nuclei (center), and lateral nuclei (right).
(G) Average width of actively transcribing region for *t48-optimizedDl2>MS2-yellow* (blue), *t48-optimizedDl1>MS2-yellow* (red), and *t48-optimizedZld>MS2-yellow* (green) over NC14.
(H-J) (H) Snapshot of *t48-Dldeletion >MS2-yellow* embryo showing false-color of all actively transcribing nuclei. (I) Average total mRNA production, (J) Average trajectory of *t48-WT* (black) and *t48-Dldeletion* (gray) *>MS2-yellow* embryos over NC14 of ventrally located nuclei.1840 and 1608 nuclei were examined from three biological replicate embryos of *t48-optimizedDl2>MS2-yellow* and *t48-Dldeletion >MS2-yellow*, respectively. All error bars shown in (C-F) and (I-J) are standard error of the mean. Error bars in (G) are standard deviation.

Figure S3

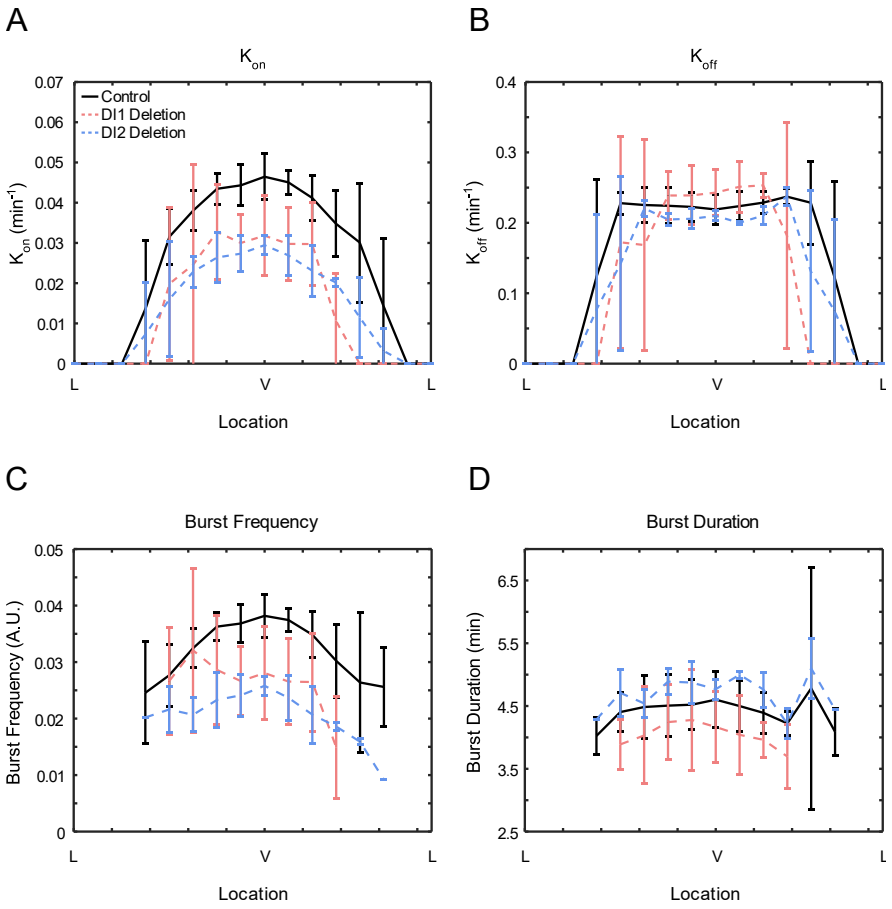

(A-D) Calculated values of k_{on} (A), k_{off} (B), burst frequency (C), and burst duration (D) across the DV axis of *MS2-yellow* reporter gene trajectories driven by *t48-WT* (black), *t48-Dl1deletion* (light red), and *t48-Dl2deletion* (light blue) enhancers. All error bars are standard deviation.

Table S1.

Primers	
t48int1Enhfwd1	TTAAGCGGCCGCCCGGCGTGCATTTGTGTTTGTTTC
t48int1Enhfwd3	TTAAGCGGCCGCGCGAAACCCACATGTTGTTCATTCTG
t48int1rev2	TTAAGCTAGCTGGGTTCCAAACATTTCCTGTC
t48int1rev3	TTAAGCTAGCAAACGAGCCCACGAGAAATCC
t48dl1optfwd	AATTCCCACCGGGGGAATTCCCGTGGGCTCGTTTTCAT
t48dl1optrev	ATGAAAACGAGCCCACGGGAATTCCCCCGGTGGGAATT
t48dl2optfwd	AGGGGCTTATTGGGGGAATTCCCTTGATTCCCTAATT
t48dl2optrev	AATTAGGGAATCAAGGGAATTCCCCCAATAAGCCCCT
t48dl1delfwd	AATTCCCACCGCTTGATTTCTCGTGGGCTC
t48dl1delrev	GAGCCCACGAGAAATCAAGCGGTGGGAATT
t48dl2delfwd	GGGGCTTATTGTGTTATTTCTTTTGATTCCCT
t48dl2delrev	AGGGAATCAAAAGAAATAACACAATAAGCCCC
t48consensuszldfwd	CGCACGCAGAACTACCTGCCTCTGGCCATCCCGCTTGCAC
t48consensuszlldrev	GTGCAAGCGGGATGGCCAGAGGCAGGTAGTTCTGCGTGCG

Movie S1.
Live imaging of (left) *t48>MS2-yellow*, (center) *t48-Dl1deletion>MS2-yellow*, and (right) *t48-Dl2deletion>MS2-yellow* embryo. Max projection of each embryo from beginning of NC14 to gastrulation. MCP-GFP is shown in green and His2Av-mRFP is shown in red. Anterior is to the left and ventral midline is along the main diagonal.

Movie S2.
Live imaging of (left) *t48>MS2-yellow*, (center) *t48-optimizedDl1>MS2-yellow*, and (right) *t48-optimizedDl2>MS2-yellow* embryo. Max projection of each embryo from beginning of NC14 to gastrulation. MCP-GFP is shown in green and His2Av-mRFP is shown in red. Anterior is to the left and ventral midline is along the main diagonal.

Movie S3.
Live imaging of (left) *t48>MS2-yellow* and (right) *t48-optimizedZld>MS2-yellow* embryo. Max projection of each embryo from beginning of NC14 to gastrulation. MCP-GFP is shown in green and His2Av-mRFP is shown in red. Anterior is to the left and ventral midline is along the main diagonal.

Movie S4.
Live imaging of (left) *t48>MS2-yellow*, (center) *t48-Dldeletion-optimizedZld>MS2-yellow*, and (right) *t48-Dldeletion >MS2-yellow* embryo. Max projection of each embryo from beginning of NC14 to gastrulation. MCP-GFP is shown in green and His2Av-mRFP is shown in red. Anterior is to the left and ventral midline is along the main diagonal.